Swells Modulated TCs Waves in the Bay of Bengal

Yongheng Zhang[1], Hui Shi[1,2,*], Yelong Chang[3,4]
[1]China Water Resources Pearl River Planning Surveying & Designing CO., LTD, Guangzhou, Guangdong, China
[2]School of Marine Sciences, Sun Yat-Sen University, Guangzhou, Guangdong, China
[3]South China University of Technology, Guangzhou, Guangdong, China
[4]South China Sea Institute of Oceanology, Chinese Academy of Sciences, Guangzhou, Guangdong, China
**Corresponding Author.*

Abstract: Tropical cyclones (TCs) waves have a significant impact on offshore and coastal engineering, beach erosion and flooding in coastal areas. An attempt is made to study the modulation effects of the swells from Southern Indian Ocean on TC waves in Bay of Bengal (BoB). The third generation ocean wave model, SWAN (Simulating Waves Nearshore) is implemented and validated to simulate significant wave heights (SWH) and mean wave period (MWP) during four TCs in 2013. Simulations were carried out by three different model domains for analyzing the swells modulation effects. It was discovered that swells from the Southern Indian Ocean significantly influence the wave climate in the Bay of Bengal during tropical cyclones. Along the western and eastern coasts of the Bay of Bengal, the contribution of swells to tropical cyclone wave heights is substantial, owing to the shelter provided by topographical features such as islands and reefs. In the inlet of the BoB, TC waves are also modulated by swells. However, near the centers of TCs and in the middle of the BoB, the modulating effects of swells are weak or even negligible.

Keywords: Wave Modeling; Swells; Bay of Bengal; Tropical Cyclones; Ocean Wave; SWAN

1. Introduction

In general, ocean waves are composed of wind seas, created by local winds, and swells, which originate from distant winds or storms. Swells, typically characterized by longer periods, possess substantially more energy than shorter wind seas, resulting in greater destructive power. Numerous studies [1-3] have determined that swells from the Southern Indian Ocean are crucial in shaping the wave climate of the Northern Indian Ocean. Specifically, the Bay of Bengal (BoB), located in the Northern Indian Ocean, is significantly influenced by these swells [4-6]. Alves concluded that the wave field in the BoB can be influenced by swells from both the Southern Indian Ocean and the South Atlantic, although the effect from the South Atlantic is relatively minor [3]. Notably, during the southwest summer monsoon, the influence of swells on the local wave climate in the Bay of Bengal diminishes.

The modulation effects of swells on the local wave climate are critically important for oceanographic studies and engineering applications. Through statistical analysis, their results indicated no significant influence of swells on the growth of wind seas. However, Alves suggested that the presence of swells impacts several critical processes at the air-sea interface, including the modulation, and suppression of short wind-generated waves [3]. Numerous studies have reported on swell propagation and the mechanisms by which swells modulate wind seas. Nevertheless, the aforementioned studies primarily focus on large regional and long-term wave climate assessments. In reality, large waves generated during tropical cyclones (TCs) in BoB also pose significant threats to coastal structures and populations, in addition to swells. The east coast of India encounters numerous low-pressure systems and about 5 to 6 tropical cyclones each year originating from the BoB, with the frequency and

intensity of these storms increasing in recent years [7,8].

This study aims to examine the modulation effects of swells from the Southern Indian Ocean on tropical cyclone waves in the Bay of Bengal. To characterize sea states during TC, the numerical wave modeling technique was used [9]. SWAN wave model has been widely used for TCs or typhoon waves. In the present study, three SWAN wave models were used by different the swell generating areas to evaluate the modulation effects of swell to TC waves.

The paper is structured as follows: Section 2 describes the data used. Section 3 discusses the variability of the wave model in the Bay of Bengal, and Section 4 examines how swells modulate tropical cyclone waves in the Bay of Bengal. The paper concludes with remarks and suggestions for future research in Section 5.

2. Data Used

2.1 Wave Data

The study utilizes measured wave data collected at a water depth of 15 meters (80.574°E, 5.934°N) off Matara, Sri Lanka (Figure. 1) using a moored wave buoy from September 2013 to February 2014 to compare with the SWAN model. The wave buoy records wave parameters, including SWH and MWP, using a pressure sensor. Pressure data are recorded continuously at a rate of 1 Hz, aggregated into 10-minute intervals, with each 30-minute period processed as a single record.

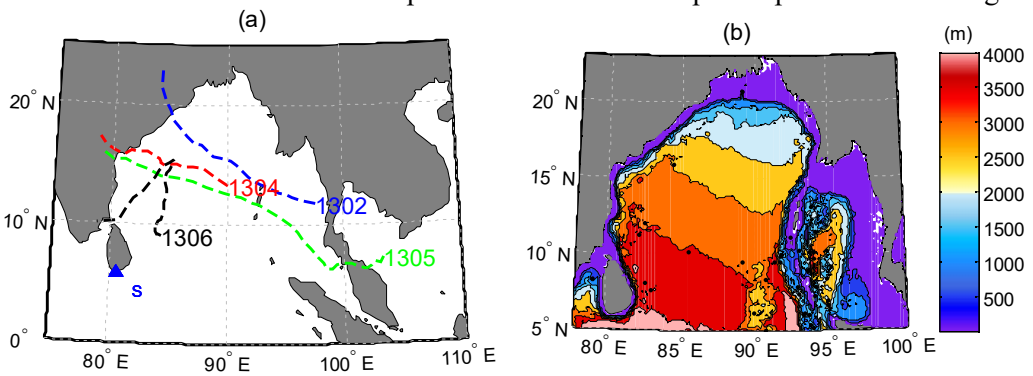

Figure 1. TCs' Track and Seafloor Topography
(a). TCs' Track and the Buoy (S) Location are Also Shown
(b). Bathymetry (in Meters) of the Nested Region N

Due to the buoy S located in the inlet of BoB, so we must get the wave data in the middle of BoB for a more effective validation of the tropical storms wave model. At present, SWH measurements of altimeters were proven accurate by comparison with buoys over the global ocean. Currently, numerous altimeters (such as Jason-2, CRYOSAT-2, and HY-2) are in orbit providing SWH data. The Jason-2 altimetry Geophysical Data Record (GDR) includes 254 passes per cycle, evenly split between 127 ascending and 127 descending passes, providing comprehensive coverage of BoB (Figure. 2). The along-track SWH data from Jason-2 used in this study were obtained from AVISO/CNES. All along-track SWH data analyzed in this study originate from the Ku-band radar altimeter aboard the satellite.

2.2 Wave Model

The SWAN model, developed by TU Delft, is a third-generation numerical model used for wave spectral modeling. Utilizing a nested mesh framework, it is particularly well-suited for nearshore applications. The model simulates wave growth through wind wave generation, nonlinear wave-wave interactions, energy dissipation due to breaking, friction, and frequency shifting caused by currents and local topographical conditions.

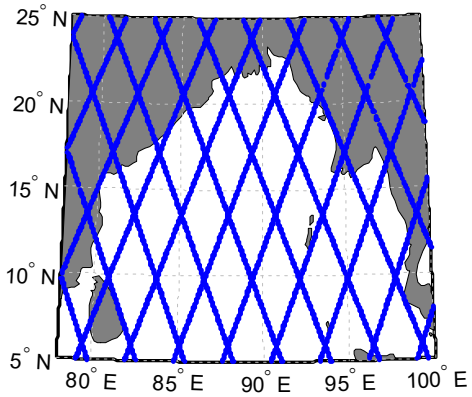

Figure 2. Track of Jason-2 in the Bay of Bengal

The evolution of the SWAN wave spectrum can be described by the spectral action balance equation, expressed as follows.

$$\frac{\partial}{\partial t}N+\frac{\partial}{\partial x}c_xN+\frac{\partial}{\partial y}c_yN+\frac{\partial}{\partial \sigma}c_\sigma N+\frac{\partial}{\partial \theta}c_\theta N=\frac{S}{\sigma}(1)$$

In Eq. (1), the source term represents generation, dissipation, and nonlinear wave-wave interactions. The SWAN model utilized in this study is appropriate for examining the nonlinear interaction processes between swells and wind waves.

2.3 Wind Forcing Module

Wave models are highly sensitive to the details of the input wind; only high-quality wind data can accurately reproduce the actual wave climate. In BoB, where the wave climate is dominated by swells, the accuracy of wave model outputs during tropical cyclones (TCs) depends on the quality of both the TC wind field and the external wind field for swells. Many analyzed surface wind fields (NECP, CCMP) were provided by research institutions. But near the center of TCs, analyzed surface wind fields have less resolution or less wind speed [4], so a high quality blended surface wind field, combining the TCs' wind model and an analyzed wind field, was used in the present study. For a relatively smooth transition between both wind fields, Carr and Elsberry provide the solution [10]:

$$V_{bl}=(1-\varepsilon)*V_{10}+V_{en} \quad (2)$$

$$\varepsilon=\frac{c^4}{1+c^4}, c=r/(nR_{max}) \quad (3)$$

where V_{bl} is the blended surface wind field, Ven is the outer wind field. V_{10} is TCs wind field, the parameter R_S is a scaling factor that can be adjusted to achieve the desired radius of maximum winds R_{max}.

A high quality analyzed surface wind field CCMP V2.0 provided by RSS is used in the present study. CCMP V2.0 gridded surface vector winds are produced using model wind data, satellite, and moored buoy. This product is classified as a wind analysis, spanning from July 1987 to the present, and serves as a continuation of the widely utilized original CCMP product. It provides an ocean surface winds, with a spatial resolution of 0.25° latitude by 0.25° longitude. Further details about this wind dateset can be found in Atlas et al [4].

To obtain the wind field associated with TCs, a stationary symmetric wind profile model is employed. Various parametric wind models have been utilized to improve the quality of wind field simulations. Here, a dynamic wind model was employed to derive the wind field at the sea surface. The Jele model assumes an exponential pressure distribution form, expressed as

When $0\leq r\leq R_w$,

$$P_a=P_0+0.25*\left(\frac{r}{R}\right)^3(P_\infty-P_0) \quad (4)$$

When $R_w\leq r\leq \infty$,

$$P_a=P_0+\left(1-\frac{3R_w}{4r}\right)(P_\infty-P_0) \quad (5)$$

in which, P_∞(1013hPa) represents the environmental pressure far from the center, P_0 denotes the central pressure of the typhoon, and r and R_w signify the radial distance from a station to the typhoon center and the radius of maximum wind speed around the typhoon center, respectively.

3. Model and Validation

3.1 Model and Method

In the present study, SWAN model is applied for three different domains along the latitude of Indian Ocean to simulate the swells with a multi-scale nested approach during TCs in all BoB. To achieve this, three distinct model domains were employed to forecast the impact of long swells reaching the Bay of Bengal, as depicted in Figure 3. These three outer domains (D1, D2, and D3) consist of finite difference coarse grids that extend respectively up to 60° S, 40° S, and 0°. They are D1(30° E-120° E, 60° S-30° N), D2 (30° E-120° E, 40° S-30° N) and D3 (30° E-120°E, 0°N-30°N) respectively. The three outer domains all nested a fine grid domain N (78°E-100°E, 5°N-23°N).

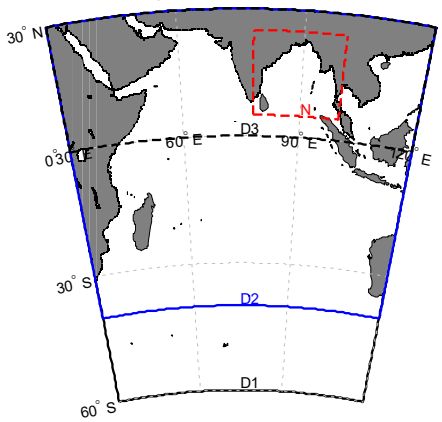

Figure 3. Multi-scale Model Domains for the Numerical Experiment (D1, D2, D3—Coarse Grid; N—Fine Grid)

Table 1. MSLP-Minimum Sea Level Pressure and VMAX-Maximum Sustained Wind Speed

TCS	MINIMUM OF MSLP (HPA)	TIME	THE CENTER OF TC	VMAX (M/S)	LEVEL OF TC DEVELOPMENT
1302	918	2013101112	16.7°N, 87.7°E	72.0	Super Typhoon
1304	970	2013112106	15.9°N, 83.3°E	36.0	Typhoon
1305	967	2013112518	12.3°N, 91.2°E	38.6	Typhoon
1306	974	2013120800	11.9°N, 84.5°E	33.4	Typhoon

In the study period, four cyclone events are analyzed for validation of wave model: TC1302 (2013/10/07 12-2013/10/13 12), TC1304 (2013/11/18 00-2013/11/23 06), TC1305 (2013/11/19 18-2013/11/29 00) and TC1306 (2013/12/05 00-2013/12/12 18). In this study, their best track message files are from JTWC, which are shown in Figure 1 & Table 1. Because distant swells require a considerable amount of time to travel to the BoB, a spin-up period of 15 days is incorporated into each simulation run. This ensures that all swell systems, which have a long residence time, are adequately captured, thereby preventing the model results from being influenced by initial conditions.

The gridded bathymetry for the study area is derived from the GEBCO database. It provides a global 30 arc-second grid generated by integrating quality-controlled depth sounding survey data with satellite-derived gravity data. Figure 2 illustrates bathymetry data for the BoB region.

Using available wave buoy data during the study period, comparisons are conducted between buoy and model in the BoB from September 2013 to February 2014. Model performance is evaluated by comparing simulated SWH and MWP with buoy observations. To quantify model performance, several output metrics are employed to assess model accuracy over time. These metrics include mean error (bias), RMSE, SI, and Pearson correlation coefficient (r). These statistical measures gauge the quality of wind forcing and the performance of the wave model relative to the corresponding buoy observations, calculated as

$$\bar{\delta} = \frac{1}{n}\sum_{i=1}^{n} \frac{abs(H_{ci}-H_{obi})}{H_{obi}} \text{(RMSE)} \quad (6)$$

$$\text{SI} = \frac{1}{\overline{H_{Ob}}}\sqrt{\sum_{i=1}^{n}\frac{1}{n}(H_{ci}-H_{obi})^2} \quad (7)$$

$$\text{r} = \frac{\sum_{i=1}^{n}(H_{ci}-\overline{H_c})(H_{obi}-\overline{H_{ob}})}{\sqrt{\sum_{i=1}^{n}(H_{ci}-\overline{H_c})^2}\sqrt{\sum_{i=1}^{n}(H_{obi}-\overline{H_{ob}})^2}} \quad (8)$$

where H_{ob} is the measured value and H_c is the modeled value, n is the total number of data, $\overline{H_{ob}}$ and $\overline{H_{ob}}$ are the mean of H_{ob} and H_c respectively.

3.2 Model Validation

Validating the SWAN model against observational data at a specific location is a crucial for the accurate development of wave hindcasts and analyses. Using available buoy data during the study period, wave characteristics derived from the SWAN model are compared with observations at a buoy location off the southern coast of Sri Lanka (denoted as S) from September 2013 to February 2014. Model performance is assessed by comparing simulated SWH and MWP with buoy measurements.

Figure 4(a) illustrates the comparison of SWH between observational data and model outputs from three coarse models, D1, D2, and D3. The comparison indicates that wave heights derived from model D1 closely match the observed wave heights. Qualitatively, the wave heights during TCs obtained in this study are consistent with those observed at the buoy location. However, it is noted that models D2 and D3 are able to reproduce both the lows and highs of wave heights at the buoy location. Additionally, wave heights from model D3 are lower than those from D2. Hence, during TCs, the contribution of Southern Indian Ocean swells to SWH in the BoB is evidently significant.

The comparison of mean wave period between observation and model output is shown in Figure 4(b). In three models, the simulated MWP shows a constant negative bias throughout the simulation period. Besides the lower spatiotemporal resolution, relaxation of CCMP V2.0, the model its limitations will leads to underestimate the mean wave period. But we can see that the changing trends from D1 get closer to observation by D2 and D3.

The detailed statistics of the validation on SWH & MWP are presented in Table 2& Table 3 respectively. D1 simulation of SWH are highly correlated (r=0.86~0.96) with in-situ measurements except TC1306 and virtually, for TC1306, there is small bias and RMSE is

only 0.11 (Figure 4 (a)). During TC1306, the SWH and MWP is closed. This showed that the propagated intensity of swells from westerlies (40S-60S) is low, and reduce its modulation effects to BoB wave climate. For MWP, the similar characteristics can be observed.

The buoy S is off the south of Sri Lanka, which is situated in the entrance to BoB and far away from the center of TCs. So a comparison of SWH also is made between Jason 2 and model as shown in Figure 5. The analysis results are almost in agreement with the conclusions obtained from the upward analysis.

The black circle represents the buoy observation value; the blue dotted line represents the model D1 result; the red dotted line represents the model D2 result; the green solid line represents the model D3 result.

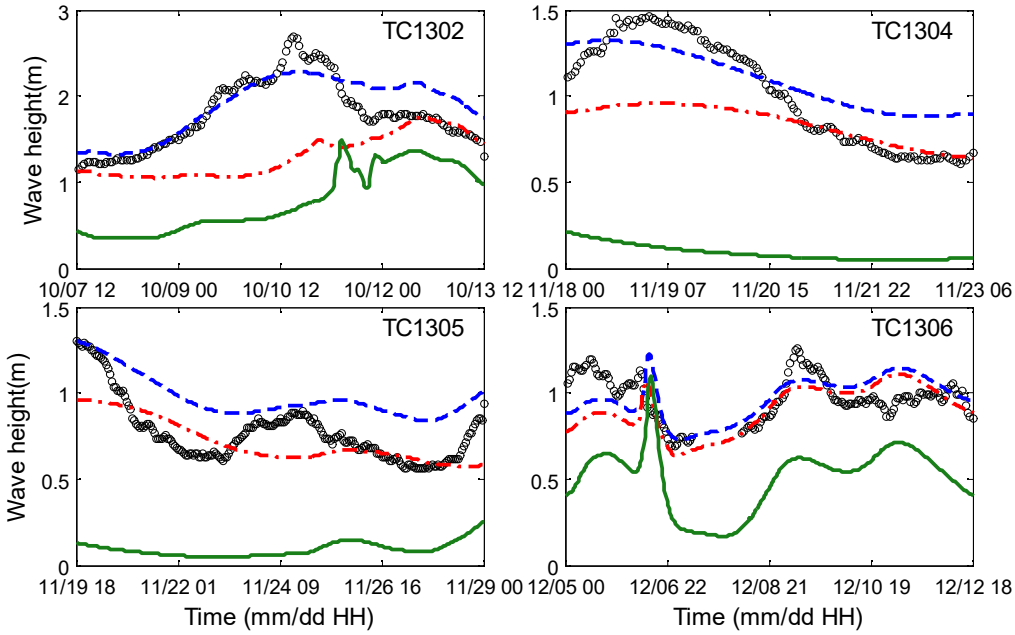

(a). Comparison of Model Results and Observational Data for Significant Wave Height at Location S

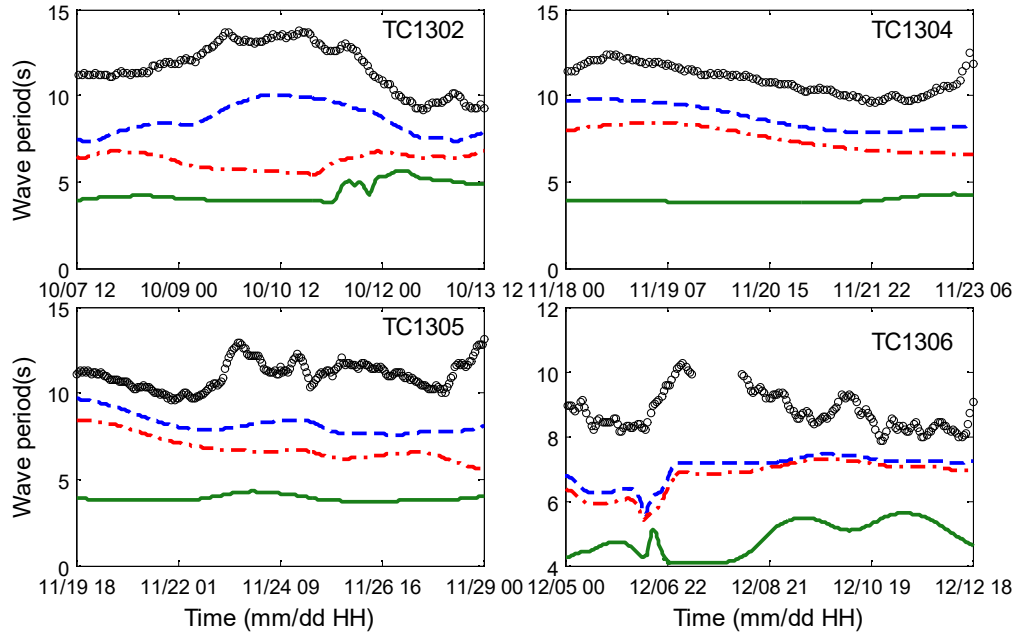

(b). Comparison of Model Results and Observational Data for Significant Wave Period at Location S.

Figure 4. Comparison of Model Results and Observational Data for Significant Wave Height (a) and Period (b) at Location S.

Table 2. Error Analysis for SWH

TC		Mean		SI	RMSE	r
		Buoy	Model			
1302	D1	1.79	1.89	0.13	0.11	0.86
	D2		1.30	0.37	0.25	0.15
	D3		0.78	0.63	0.56	0.22
1304	D1	1.03	1.09	0.16	0.18	0.96
	D2		0.84	0.27	0.17	0.95
	D3		0.09	0.95	0.91	0.75
1305	D1	0.77	0.97	0.29	0.29	0.87
	D2		0.74	0.19	0.14	0.65
	D3		0.09	0.91	0.88	0.14
1306	D1	0.98	0.99	0.14	0.11	0.41
	D2		0.93	0.15	0.11	0.42
	D3		0.55	0.46	0.45	0.48

Table 3. Error Analysis for MWP

TC		Mean		SI	RMSE	r
		Buoy	Model			
1302	D1	11.69	8.63	0.27	0.26	0.86
	D2		6.22	0.49	0.46	-0.78
	D3		4.39	0.64	0.61	-0.77
1304	D1	10.94	8.73	0.20	0.20	0.92
	D2		7.54	0.31	0.31	0.83
	D3		3.92	0.65	0.64	-0.12
1305	D1	11.06	8.17	0.28	0.26	-0.06
	D2		6.82	0.40	0.38	-0.38
	D3		3.89	0.65	0.65	0.50
1306	D1	8.74	6.98	0.22	0.20	0.13
	D2		6.75	0.24	0.22	0.07
	D3		4.94	0.45	0.43	-0.53

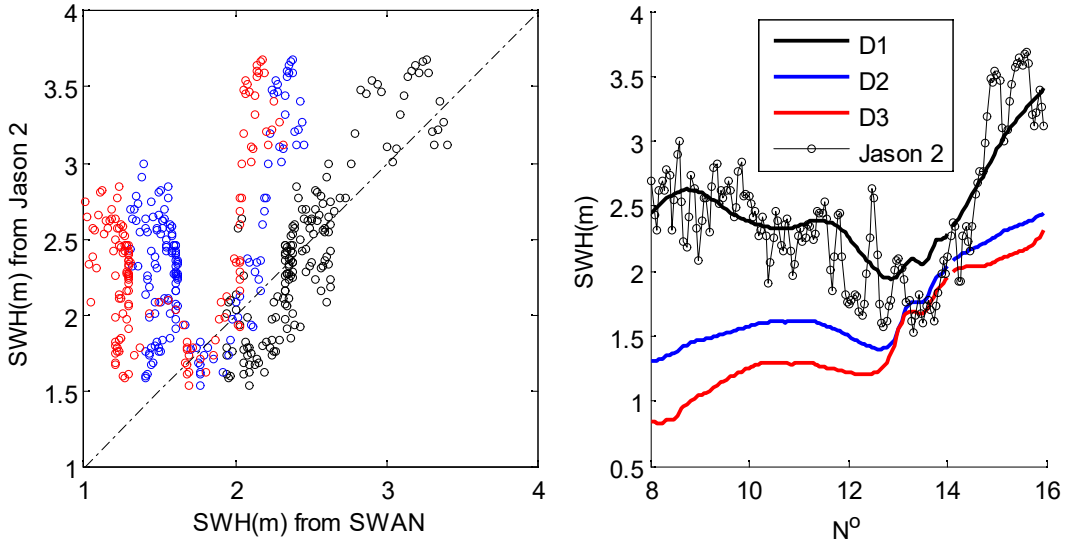

Figure 5. Scatter Plots of Collocated SWH Observations for Jason 2 and Simulation for SWAN during TC 1302

4. Modulation of Swells on Wave Climate during TCs

To estimate the Southern Indian Ocean swells modulation effects to the wave climate in BoB during TCs, the wave parameters are obtained from the three simulations D1, D2 and D3. It is anticipated that the wave heights measured by D3 show little to no contribution from swells originating in the Southern Ocean. But the situation is the opposite for D1, and D2 is intermediate state. Table 1 shows that TC1302 is only super typhoon, and the maximum of VMAX is 72m/s, over twice as big as the other three TCs. In this section, an attempt was made for the modulation effects of swells during TC1302.

We can be seen from the above analysis that influence of swells from South Indian Ocean for BoB wave distribution is huge. During TC 1302, the swells generated in south of 40°S is about 50% percent of SWH at S (Figure. 1). The wave distribution of TC1302 at three different time is shown in Figure 6.

In the contours of column (ii) and (iii), the larger value of contours, the greater influence of swells. For simulation SWH from D1, D2 and D3, in the area protected by topography (islands and reefs et al.), the influence of swells is greater. The results are in agreement with the swells' character. The swells, because of longer wave length, can spread easily behind obstacles. In general, there is a strong wave area in the right side of center of TC in the Northern Hemisphere. In the strong wave area (in column (i) of Figure. 6), the swells have smaller impact as shown in Figure. 6.

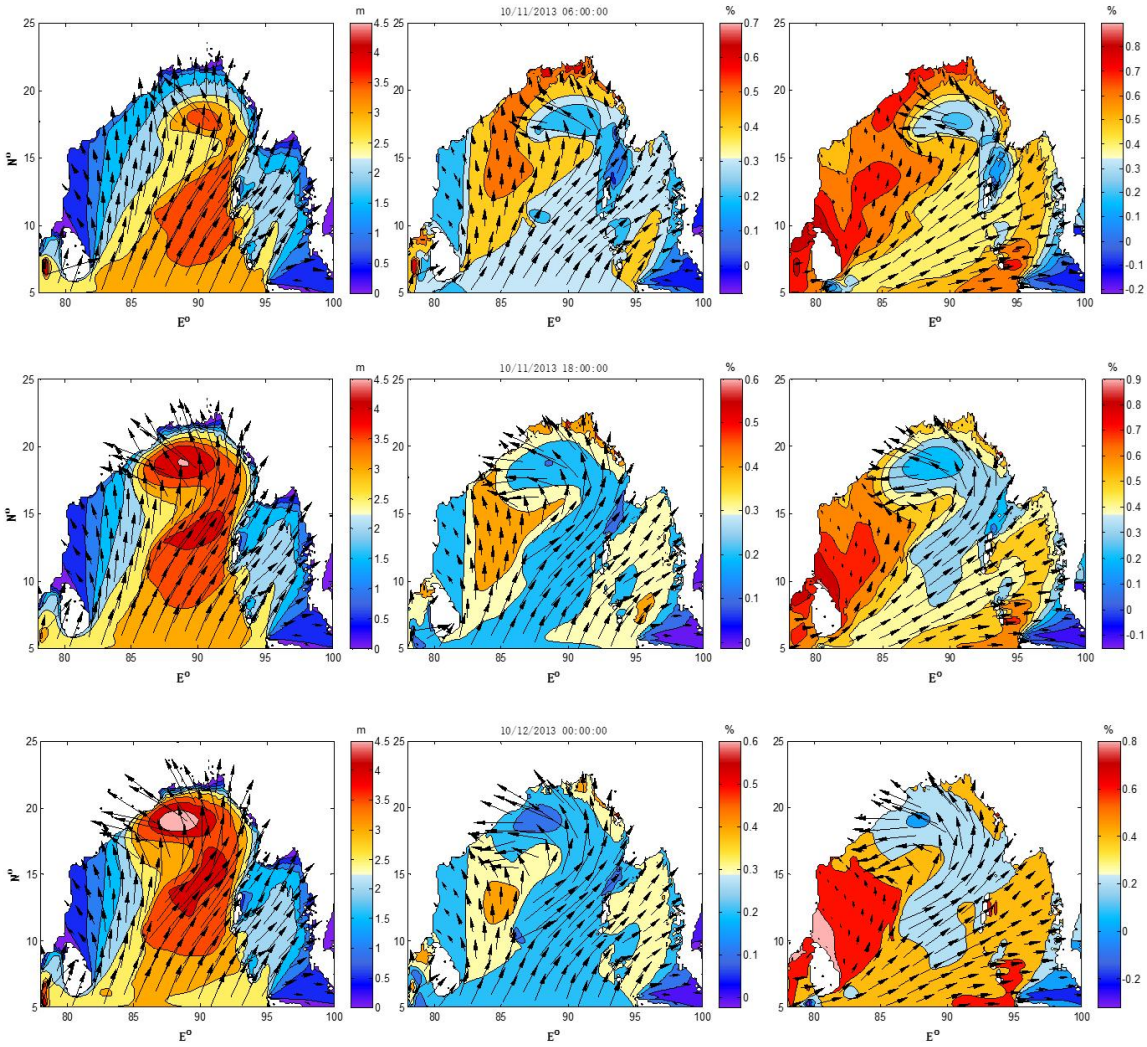

(i) (ii) (iii)

Figure 6. The Wave Distribution of TC1302
(i). SWH H1 contours of D1, (m)
(ii). $\frac{H_1-H_2}{H_1}$ contours, (%), in which H2 is SWH of D2
(iii). $\frac{H_1-H_3}{H_1}$ contours, (%), in which H2 is SWH of D2

Notes: The arrows represents wave vectors of D1, D2 and D3 respectively in columns (i), (ii) and (iii). Contours.

On comparing the three simulations, it can be known that how the swells modulated the wave climate from local winds during storm cyclones. During TC1302, in the mouth of BoB, except the SWH is larger from D1 than D3, the main wave direction (MWD) a minor shift to the west from D1 to D2 and D3. This is clear evidence for modulation of swells to TC wave climate. But near the center of TC, the modulation effects of the swells on SWH and MWD is weak or no.

5. Conclusion

This paper attempts to reveal the modulation effect of South Indian Ocean swell on TC waves through the numerical model SWAN. The third generation ocean wave model SWAN has been implemented well and validated to provide wave hindcast during four TCs in 2013 for the BoB using the mixed winds with CCMP analyzed wind speeds and wind model. In order to analyze the impact of swells generated in different regions on TC waves in the BoB, we set up three models with different calculation areas: D1, D2 and D3. D1 including the all Indian Ocean over 60°S–30°N, and D2 over 40°S–30°N region which let swells freely propagate into the Northern Indian Ocean. The third simulation D3 with winds over 40°S–0°N region was considered to

only generate local wind wave.

Comparing the three simulations provides insight into the contribution of swells from Southern Indian Ocean in the Northern Indian Ocean. The swells generated in south of 40 S is most important for the all BoB wave distribution simulation during TCs. Take Typhoon 1302 as an example. The swells in the D2 area can have an impact of about 20% on the typhoon wave SWH in the BoB area, and the swells generated in the D3 area can have an impact of about 30%. But near the center of TC, the modulation effects of the swells on SWH and MWD is weak or no.

References

[1] Aboobacker VM, Rashmi R, Vethamony P, Menon HB, 2011a. On the dominance of pre-existing swells over wind seas along the west coast of India. Cont. Shelf Research 31, 1701–1712.

[2] Aboobacker VM, Vethamony P, Rashmi R, 2011b. Shamal swells in the Arabian Sea and their influence along the west coast of India. Geophysical Research Letters. 38 (3), 7.

[3] Alves Jose-Henrique GM (2006). Numerical modeling of ocean swell contributions to the global wind-wave climate. Ocean Modelling, 11(1–2), 98-122.

[4] Atlas R, Hoffman RN, Ardizzone J, Leidner SM, Jusem JC, Smith DK, et al. (2011). A cross-calibrated, multiplatform ocean surface wind velocity product for meteorological and oceanographic applications. Bulletin of the American Meteorological Society, 92, 157–174.

[5] Pierre Queffeulou. (2004). Long-term validation of wave height measurements from altimeters. Marine Geodesy, 27(3), 495-510.

[6] Ris RC, Booij N, Holthuijsen LH. (1999). A third-generation wave model for coastal regions, 2. verification. J. geophys res. 104(c4):7667-7681.

[7] Hanson JL, Phillips OM, (2001). Automated analysis of ocean surface directional wave spectra. J. Atmos. Ocean. Technol., 277–293.

[8] Houston SH, Shaffer WA, Powell MD, Chen J. (1999). Comparisons of HRD and SLOSH surface wind fields in hurricanes: implications for storm surge modeling. Weather & Forecasting, 14(5), 671-686.

[9] Kim SY, Yasuda T, Mase H. (2008). Numerical analysis of effects of tidal variations on storm surges and waves. Applied Ocean Research, 30(4), 311-322.

[10] Glejin J, Kumar VS, Nair TMB. (2013). Monsoon and cyclone induced wave climate over the near shore waters off puduchery, south western bay of bengal. Ocean Engineering, 72(4), 277-286.

